12th IFAC International Symposium on
Advanced Control of Chemical Processes
July 14-17, 2024. Toronto, Canada

Controlling Paracetamol Unseeded Batch Crystallization with NMPC and Inverse Model

Fernando Arrais R. D. Lima * **Marcellus G. F. de Moraes** **
Martha A. Grover *** **Amaro G. Barreto Jr.** *
Argimiro R. Secchi **** **Maurício B. de Souza Jr.** *

* *Escola de Química, EPQB, Universidade Federal do Rio de Janeiro, P.O. Box 68542, Rio de Janeiro, RJ 21941-909, Brazil (e-mail: farrais@eq.ufrj.br, amaro@eq.ufrj.br, mbsj@eq.ufrj.br).*
** *Rio de Janeiro State University (UERJ), Rua São Francisco Xavier, 524, Maracanã, Rio de Janeiro, RJ 20550-900, Brazil (e-mail: marcellus@peq.coppe.ufrj.br)*
*** *School of Chemical & Biomolecular Engineering, Georgia Institute of Technology, 311 Ferst Dr. NW, Atlanta, GA, 30332-0100 USA (e-mail: martha.grover@chbe.gatech.edu)*
**** *Programa de Engenharia Química, PEQ/COPPE, Universidade Federal do Rio de Janeiro, P.O. Box 68502, Rio de Janeiro, RJ 21941-972, Brazil (e-mail: arge@peq.coppe.ufrj.br)*

Abstract: In this work, two model-based controllers were developed, one based on a nonlinear model-based controller (NMPC) using a population balance model (PBM) and another using a machine learning approach based on a neural network inverse model-based controller (NNIMC). The performance of the two model-based controllers was compared for different scenarios to obtain optimal temperature policies for controlling the mass yield and crystals' size for the unseeded batch cooling crystallization of paracetamol. The results show that both strategies are effective for crystallization control, presenting comparable results for the controlled variables in different scenarios. The controllers were also tested by applying random noise in the state variables. In these cases, the NNIMC presented advantages in having a lower computational cost for optimum control action calculations and less control effort regarding the manipulated variable's variation to reach values for the control variables at the end of the batch close to the NMPC and the setpoints.

Keywords: Neural networks, Model predictive control, NNIMC, Machine learning, Batch process control, Noise

1. INTRODUCTION

Crystallization processes are applied in separating and purifying substances, especially in the pharmaceutical and food industries. The understanding of the underlying processes and their sensitivity to the operating parameters are key aspects to meet product specifications and production yield targets (Nagy and Braatz, 2012; Lewis *et al.*, 2015). However, crystallization processes exhibit complex nonlinear behavior, requiring advanced modeling frameworks like population balances. These models often involve estimating multiple parameters from experimental data, a challenging task due to the diverse range of crystallization setups and operating conditions (Nagy, 2009).

Ensuring control over crystal size, shape, and mass yield is essential in industrial crystallization. Concerning the control of crystallization processes, there have been different proposed control strategies, such as PID and model-based controllers (Nagy, 2009; Jha *et al.*, 2017; Moraes *et al.*, 2018; Grover *et al.*, 2020). In model-based control schemes, the adoption of Model Predictive Control (MPC) becomes feasible and more appealing when the output variables, such as solute concentration and crystal size distribution, can be measured and monitored (Lima *et al.*, 2022; Kalbasenka *et al.*, 2012).

Nagy and Braatz (2003) introduced a Nonlinear Model Predictive Control (NMPC) approach, explicitly addressing parameter uncertainty to enhance the robust performance of state estimation in batch processes. Furthermore, NMPC has been employed in the polymorph control of the L-glutamic acid system (Hermanto *et al.*, 2011). Szilágyi *et al.* (2018) have developed an NMPC specifically designed to control the chord length distribution. Wang *et al.* (2023) proposed an NMPC for crystal size online control of alum crystallization, showing better performance when compared to model-free approaches.

Another noteworthy approach in establishing model-based control policies is the dynamic programming method, which allows the offline calculation and storage of con-

trol input policies. Empirical models, such as the Markov State Model based on experimental measurements, have been utilized in the dynamic programming approach to crystallization control (Grover *et al.*, 2020). In this sense, machine learning offers a versatile and flexible alternative for modeling in this context. Data-driven approaches have been applied to chemical processes, leveraging the ability to capture intrinsic nonlinearities with low computational costs (Venkatasubramanian, 2019). Despite recent advancements in data-driven modeling, there is a noticeable gap in studies applying machine learning algorithms, especially neural networks, to control crystallization operations (Xiouras *et al.*, 2022).

Damour *et al.* (2010) employed a neural network-based NMPC for continuous sugar crystallization, using crystal mass as the controlled variable and feed mass flow rate as input. Anandan *et al.* (2022) developed a controller based on reinforcement learning for paracetamol crystallization to achieve the desired crystal size. The literature also presents hybrid modeling approaches incorporating neural networks and population balance (Meng *et al.*, 2019; Lima *et al.*, 2023a) and studies proposing NMPC approaches using recurrent neural networks for crystallization control (Zheng *et al.*, 2022a,b).

In the present work, controlling the mass and crystal size in the batch cooling crystallization of paracetamol was investigated using model-based optimal control schemes. Two approaches were developed and compared: an NMPC and a neural network inverse model-based controller (NNIMC). The population balance developed by Kim *et al.* (2023) was applied as the internal model of the NMPC (and as the plant model), and the NNIMC was obtained based on NMPC simulation datasets. Four different target specifications scenarios for the controlled batches were evaluated, and scenarios with normally distributed noise in the state variables were also considered. The NNIMC exhibited advantages, such as lower computational cost and less manipulated variable effort, especially in the cases evaluated with noise.

2. METHODOLOGY

2.1 Nonlinear Model Predictive Control

An NMPC strategy was proposed for controlling the paracetamol unseeded batch crystallization in ethanol solution. The population balance model (PBM) developed by Kim *et al.* (2023) was used as the internal model of the controller and to simulate the process. This model accounts for crystal nucleation, growth, and dissolution. Furthermore, it was solved by applying the method of moments, in which the moment is defined by:

$$\mu_i = \int_0^\infty L^i n(L)\, dL, i = 0, 1, 2, 3, ... \tag{1}$$

where μ_i is the i^{th} order moment, L is the characteristic crystal size, and $n(L)$ is the number density of crystals. The moments μ_0, μ_1, μ_2, and μ_3 are proportional to the total number, length, surface area, and volume of crystals, respectively.

The paracetamol crystallization PBM is described as

$$\frac{d\mu_0}{dt} = B_1 + B_2 \tag{2a}$$
$$\frac{d\mu_1}{dt} = G\mu_0 \tag{2b}$$
$$\frac{d\mu_2}{dt} = 2G\mu_1 \tag{2c}$$
$$\frac{d\mu_3}{dt} = 3G\mu_2 \tag{2d}$$
$$\frac{dC}{dt} = -3k_V\rho_c G\mu_2 \tag{2e}$$

where k_V is the volume shape factor and ρ_c is the solid density of crystals [g/cm^3]. These parameter values can be found in Kim *et al.* (2023). B_1 is the primary nucleation rate

$$B_1 = \begin{cases} k_{b1}\exp\left[-\dfrac{16\pi\nu^2\sigma^3}{3k^3T^3(\ln S)^2}\right], S \geq 1 \\ 0, S < 1 \end{cases} \tag{3}$$

where k_{b1} is a rate constant [(min.g solvent)$^{-1}$], σ is the interfacial energy between crystal and solution [J/m^2], k is the Boltzmann constant [m^{2}kg/(s^{2}K)], and ν is the volume of one solute molecule [m^3]. S is the supersaturation and is calculated by the ratio between the concentration in the solution C [g/g] and the saturated concentration at the system temperature C_s [g/g], as described by

$$S = C/C_s \tag{4a}$$
$$C_s = 4.590\times10^{-7}T^3 - 3.610\times10^{-4}T^2 + 9.669\times10^{-2}T - 8.707 \tag{4b}$$

where T is the process temperature [K].

B_2 is the secondary nucleation rate

$$B_2 = \begin{cases} k_{b2}\,(S-1)^\alpha\, m_s^\beta, S \geq 1 \\ 0, S < 1 \end{cases} \tag{5}$$

where k_{b2} is a rate constant [(g/kg)$^{-\beta}$/(min.g solvent)], m_s is the mass of crystals in a unit of mass solution [g/kg], α and β are model parameters (Kim *et al.*, 2023).

The growth and dissolution rates are described by

$$G = \begin{cases} k_g\exp\left(-\dfrac{E_{ag}}{RT}\right)(C - C_s)^{\gamma_g}, S \geq 1 \\ k_d\exp\left(-\dfrac{E_{ad}}{RT}\right)(C_s - C)^{\gamma_d}, S < 1 \end{cases} \tag{6}$$

where k_g and k_d are the pre–exponential rate constants for the crystal growth [(μm/min)(g solute/g solvent)$^{-\gamma_g}$] and dissolution [(μm/min)(g solute/g solvent)$^{-\gamma_d}$], respectively, E_{ag} and E_{ad} are the activation energies for growth and dissolution [J/mol], and γ_g and γ_d are exponential parameters on supersaturation for the growth and dissolution, respectively. R is the universal gas constant [J/(mol K)] (Kim *et al.*, 2023).

The NMPC aims to minimize the objective function

$$J = \sum_{e=1}^{N_{cv}}\sum_{f=k+1}^{f+P}\delta_e\left(y_e(f) - y_e^{sp}(f)\right)^2 + \sum_{a=1}^{N_{mv}}\sum_{b=k}^{k+M-1}\lambda_a\Delta u_a(b)^2 \tag{7}$$

where u_a is the manipulated variable a, y_e is the controlled variable e, y_e^{sp} is the desired value of the controlled variable e, P is the prediction horizon, M is the control horizon, and N_{cv} and N_{mv} are the number of controlled and manipulated variables, respectively. δ_e is the weight value related to the controlled variable e and λ_a is the weight value related to the manipulated variable a. In this work, the controller aims to maintain the mean volume crystal size $\bar{L}_{30}$ and the mass of crystals m by manipulating the temperature of the process. The controlled variables are described in Eqs. (8) and (9), in which $m_{solvent}$ is the mass of ethanol and was defined as 100 g according to the experiments in Kim *et al.* (2023).

$$\bar{L}_{30} = \left(\frac{\mu_3}{\mu_0}\right)^{\frac{1}{3}} \tag{8}$$

$$m = k_V \rho_c \mu_3 m_{solvent} \tag{9}$$

The initial supersaturation, the initial temperature, and the setpoints used for controlling the paracetamol crystallization are presented in Table 1. Before starting the process control, the crystallization was maintained at the initial temperature for 60 min in all cases to promote the initial growth. After that, the control is started and the process is controlled for 200 min. A sampling time of one minute was adopted. All simulations were performed with a computer having the following specifications: Intel Core i7-10700, CPU 2.9 GHz, and 16 GB of RAM.

Table 1. Setpoints used to analyze the performance of the NMPC, and initial supersaturation and temperature.

Case	$\bar{L}_{30}^{sp}$ [μm]	m^{sp} [g]	S_0	T_0 [°C]
1	225	9.0	1.35	30.0
2	200	9.0	1.35	30.0
3	175	7.0	1.30	33.4
4	160	8.0	1.28	33.4

The NMPC was implemented using the Python library built in Lima *et al.* (2023b). Therefore, the Casadi (Andersson *et al.*, 2019) software for nonlinear optimization and automatic differentiation was employed to solve the NMPC with the orthogonal collocation on finite elements approach. The interface IDAS from Casadi was used to solve the ODE system. The NMPC tuning was defined based on sensitivity analysis of the controller's performance to achieve the setpoints in Table 1, which were chosen based on the study of Kim (2021). The NMPC constraints were defined as

$$0°\text{C} \leq T(k) \leq 70°\text{C} \tag{10a}$$
$$-1°\text{C} \leq \Delta T(k) \leq 1°\text{C} \tag{10b}$$

2.2 Neural Network Inverse Model Control

With the NMPC development, some controlled batches were simulated and a neural network was built to predict the optimal temperature to achieve the setpoints of the mean volume crystal size $\bar{L}_{30}$ and the mass of crystals. This NNIMC strategy is presented in Fig 1. The neural network uses the temperature, $\mu_0, \mu_1, \mu_2, \mu_3$, the concentration, and the setpoints of the controlled variables at a time step k to predict the optimal temperature at time step $k+1$.

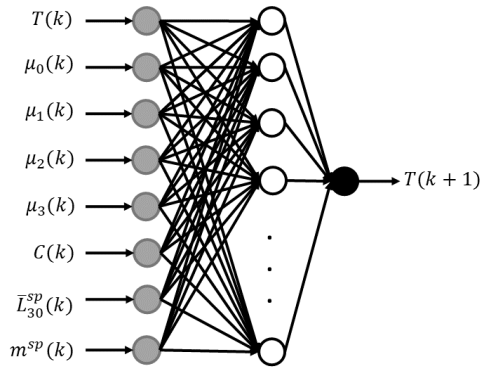

Fig. 1. Inverse model as a neural network scheme.

The neural network was trained with simulated data from the NMPC. This dataset was composed of 150 simulated crystallization batches. These batches were run considering different setpoint values and changing the initial temperature and the initial supersaturation. Moreover, the batches were run with an initial growth period of 60 min, maintaining the process at the initial temperature and then the application of the control system for 200 min to achieve the desired values of the controlled variables, considering a sampling time of 1 min. Therefore, the dataset is composed of 30,000 values of temperature, concentration, $\mu_0, \mu_1, \mu_2, \mu_3, \bar{L}_{30}$, and mass of crystals.

The neural network was built using the Keras library from Python (Chollet *et al.*, 2015). The dataset was randomly divided, of which 60% was used for training, 30% for testing, and 10% for validation. The number of hidden layers, the number of neurons, and the activation function of the hidden layers were selected using the Keras tuner to minimize the mean squared error considering the validation set. The tuner was set to find the optimal neural network composed of one to five hidden layers and 10 to 500 neurons in each layer. Also, the search region of the hidden layers' activation function was composed of ReLU, SeLU, ELU, and hyperbolic tangent. The maximum number of trials was defined as 300 in the Keras tuner. The neural networks were trained with the Adam algorithm, with a batch size of 200 and early stopping. The performance of the NNIMC was also tested for the cases presented in Table 1, and the simulations were performed on the same computer as the NMPC simulations.

The control scheme is presented in Fig. 2. The PBM developed by Kim *et al.* (2023) is used as the simulated process, making predictions of $\mu_0, \mu_1, \mu_2, \mu_3$, and the concentration for the given initial conditions. These predictions, the current temperature, and the setpoints are scaled and are introduced to the neural network. The variables are scaled in the range of 0 to 1, considering their maximum and minimum values of the entire dataset (train, test, and validation). Then, the neural network predicts the scaled value of the optimum temperature to achieve the setpoints. The temperature in the range of 0 to 1 is inverse scaled to the original temperature range and introduced to the PBM to make new predictions of the state variables according to the actual values of $\mu_0, \mu_1, \mu_2, \mu_3$, and the concentration.

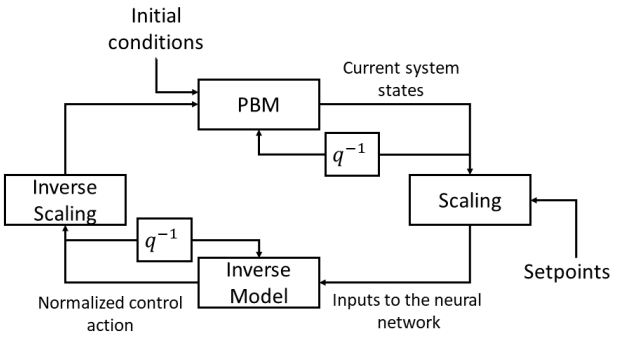

Fig. 2. NNIMC scheme, in which q^{-1} is a shift operator.

3. CONTROL ANALYSIS

The NMPC was tuned with a control horizon equal to 5 and a prediction horizon equal to 10. Moreover, δ_e was tuned as 10^{-2} for $\bar{L}_{30}$ and 1 for m, while λ_a was defined as 10^{-5}. For the NNIMC, the optimal neural network presented 4 hidden layers, each with 180 neurons, and ReLU as the activation function of all hidden layers. Table 2 presents the mean squared error (MSE), mean absolute error (MAE), and the R^2 for the training, test, and validation datasets using the optimal neural network to make predictions and considering temperature values not normalized. Therefore, the predictions of the NNIMC were very similar to the original values for the three datasets.

Table 2. Metrics values to evaluate the neural network.

Metric	Train	Test	Validation
MSE	9.297×10^{-3}	1.233×10^{-2}	8.474×10^{-3}
MAE	4.330×10^{-2}	4.686×10^{-2}	4.197×10^{-2}
R^2	0.9998	0.9997	0.9998

Table 3 presents the values of the mean volume crystal size and the mass of crystals at the end of the batch, and the sum of the squared variation of the manipulated variable, representing the total control effort, for each simulated case with both control approaches. The two strategies could reach values close to the setpoints for both controlled variables. For Case 1, the NNIMC and the NMPC presented offsets on both controlled variables. The NMPC achieved a mean volume crystal size closer to the setpoint than the NNIMC, while the opposite was observed regarding the mass of crystals. For the other three cases, the control strategies reached values of the controlled variables closer to the setpoints compared to the previous case, not presenting a significant offset. The performance of the NMPC was better than the NNIMC in Case 2, while the performance of the NNIMC was better in Cases 3 and 4. However, the performance of both control methods was similar, reaching similar values of the controlled variables at the end of each batch. Regarding the control action, both approaches proposed similar temperature values, verifying a better performance, in terms of control effort, of the NMPC in Cases 1 and 2, while the NNIMC was better in the other scenarios.

Fig. 3 presents the performance of the NMPC and the NNIMC for Case 4. The behavior of the control actions calculated by both approaches is similar. A stable temperature is maintained after the setpoints are achieved. Moreover, the NMPC and the NNIMC can achieve the setpoints immediately after the initial growth of 60 min without control and maintain the controlled variables on the desired values until the end of the batch. In Fig. 3, both strategies presented a small overshoot for the crystal mass before achieving the setpoint. Therefore, the NNIMC and the NMPC present a potential for controlling the paracetamol batch crystallization process.

Table 3. $\bar{L}_{30}$ and m values at the end of the controlled batches with the NMPC and the NNIMC, and the total control effort.

Case	System	$\bar{L}_{30}$ (μm)	m (g)	$\sum \Delta u(k)^2$
1	Target	225.0	9.00	-
	NNIMC	211.6	9.70	6.18
	NMPC	212.8	9.88	4.66
2	Target	200.0	9.00	-
	NNIMC	196.6	9.20	9.91
	NMPC	197.7	9.16	7.87
3	Target	175.0	7.00	-
	NNIMC	174.3	7.06	17.47
	NMPC	173.6	7.12	22.99
4	Target	160.0	8.00	-
	NNIMC	159.1	8.03	22.61
	NMPC	159.0	8.07	24.19

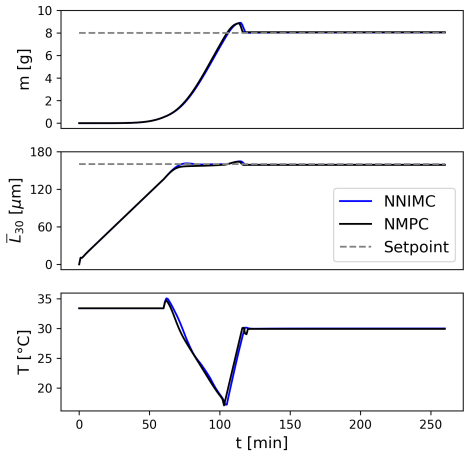

Fig. 3. Performance of the NMPC and the NNIMC for Case 4.

Table 4 presents the average time the NNIMC and the NMPC required to calculate the control actions in each case. Both approaches took around the same time to obtain these values. The NNIMC took less time to calculate the temperature in Cases 2 and 4, while the opposite happened in Cases 1 and 3. A relevant characteristic of a controller is obtaining the control action quickly in order to apply this change immediately to the process and achieve the desired values of the controlled variables without delay. Both control approaches demanded less time than the sampling time to compute a control action.

Real measurements always present uncertainties, and to account for this, we tested the performance of the controllers by applying random noise in the state variables following the normal distribution. The noise is described in (11), in which y_i^m is the state variable i (concentration and

Table 4. Mean time for the NNIMC and the NMPC to calculate the optimal control action.

Case	NNIMC time (s)	NMPC time (s)
1	4.081×10^{-2}	3.981×10^{-2}
2	4.085×10^{-2}	4.789×10^{-2}
3	4.112×10^{-2}	2.641×10^{-2}
4	4.091×10^{-2}	4.208×10^{-2}

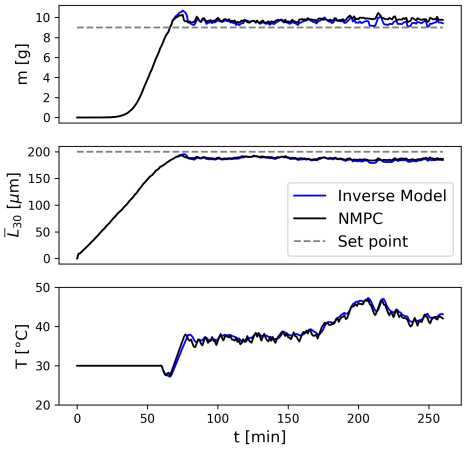

Fig. 4. Performance of the NMPC and the NNIMC for Case 2 with noise.

moments), and $R(t)$ is a random variable ($R(t) \sim N(0,1)$). Each case was simulated 300 times to test the controllers' performance with different noise values.

$$\tilde{y}_i^m = y_i^m \left(1 + 0.01R(t)\right) \tag{11}$$

The performance of the controllers for a random simulation of Case 2 with noise is illustrated in Fig. 4. In the simulations of Case 1, the controllers could not reach the setpoints again, presenting offset on both controlled variables. However, the NMPC and the NNIMC could maintain the controlled variables in their setpoints in most simulations of the other cases, even accounting for noise. Moreover, the NNIMC presented the advantage of making fewer changes in the manipulated variable. This advantage can also be seen in Table 5 , which presents the standard deviation and the mean value of the sum of the squared variation of the manipulated variable in each time step during the operation of the controllers for the 300 simulations. The NMPC imposed more temperature changes to the crystallization process compared to the NNIMC, using more energy to control the process. Furthermore, the total control effort presented high standard deviation values, showing that the noise presents a big influence on the control action, especially in the NMPC. Table 5 also presents the mean values of the mean volume crystal size and the mass of crystals at the end of the batch and their standard deviations for the 300 simulations. In most cases, the NMPC and the NNIMC could achieve similar values for the controlled variables, closely approaching the setpoints while exhibiting low standard deviation.

Table 6 presents the average time the control approach takes to calculate the control actions, accounting for the noise and 200 calculations of the control action in each simulation of a specific case. The NNIMC demanded a similar time compared to its performance, not considering noise. On the other hand, the NMPC demanded more time in comparison to the previous case. Therefore, the NNIMC presented an advantage in computational cost compared to the NMPC.

Table 5. Standard deviation and mean values of $\bar{L}_{30}$ and m at the end of the noisy controlled batches with the NMPC and the NNIMC, and standard deviation and mean of the total control effort.

Case	System	$\bar{L}_{30}$ (μm)	m (g)	$\sum \Delta u(k)^2$
1	Target	225.00	9.000	-
	NNIMC	208.16 ± 0.46	9.275 ± 0.037	17.98 ± 7.65
	NMPC	207.55 ± 0.47	9.454 ± 0.022	80.40 ± 32.83
2	Target	200.00	9.000	-
	NNIMC	192.79 ± 0.06	8.835 ± 0.012	19.89 ± 8.69
	NMPC	192.11 ± 2.17	8.61 ± 0.093	76.27 ± 56.91
3	Target	175.00	7.000	-
	NNIMC	174.62 ± 0.21	6.849 ± 0.013	30.07 ± 9.04
	NMPC	172.42 ± 0.03	7.140 ± 0.001	131.17 ± 43.91
4	Target	160.00	8.000	-
	NNIMC	158.95 ± 0.19	7.817 ± 0.001	36.39 ± 14.19
	NMPC	159.98 ± 0.23	8.013 ± 0.001	120.09 ± 51.30

Table 6. Mean time for the NNIMC and the NMPC calculate the optimal control action 200 times in each case with noise in the state variables.

Case	NNIMC time (s)	NMPC time (s)
1	4.087×10^{-2}	1.007×10^{-1}
2	4.059×10^{-2}	9.375×10^{-2}
3	4.057×10^{-2}	1.345×10^{-1}
4	4.063×10^{-2}	1.270×10^{-1}

4. CONCLUSION

This work aimed to show the potential application of neural network-based control of a batch cooling crystallization process. This proposed controller considered this machine learning tool as an inverse model, that is an NNIMC, and its performance was compared to a nonlinear model predictive controller (NMPC) for controlling the yield and size of the crystals. The neural network training, testing, and validation showed predictions very close to the true values for the respective datasets obtained from the NMPC simulated data. Comparing the performances, the NNIMC showed a lower computational cost in the evaluated scenarios accounting for noise. Another advantage of the NNIMC is that it imposed fewer temperature changes than the NMPC, using much less energy to achieve the same control target. In this way, the machine learning approach proved to be a good alternative to the NMPC, which uses the population balance model as an internal model. The introduction of noise into the process suggests that, for practical applications of crystallization control, the NNIMC presents greater versatility.

ACKNOWLEDGEMENTS

The authors acknowledge funding from the Brazilian Coordination for the Improvement of Higher Education Personnel (CAPES, Finance Code 001), the National Council for

Scientific and Technological Development (CNPq, Grants 303587/2020-2, 311153/2021-6, and 313337/2021-7), and the Research Support Foundation of the State of Rio de Janeiro (FAPERJ, Grants E 26/111.671/2013 and E-26/201.148/2022).

REFERENCES

Anandan, P.D., Rielly, C.D., and Benyahia, B. (2022). Optimal control policies of a crystallization process using inverse reinforcement learning. In *Computer Aided Chemical Engineering*, volume 51, 1093–1098. doi: https://doi.org/10.1016/B978-0-323-95879-0.50183-1.

Andersson, J.A.E., Gillis, J., Horn, G., Rawlings, J.B., and Diehl, M. (2019). CasADi – A software framework for nonlinear optimization and optimal control. *Mathematical Programming Computation*, 11(1), 1–36. doi: https://doi.org/10.1007/s12532-018-0139-4.

Chollet, F. *et al.* (2015). Keras. `https://keras.io`.

Damour, C., Benne, M., Boillereaux, L., Grondin-Perez, B., and Chabriat, J.P. (2010). Nmpc of an industrial crystallization process using model-based observers. *Journal of Industrial and Engineering Chemistry*, 16(5), 708–716. doi:https://doi.org/10.1016/j.jiec.2010.07.014.

Grover, M.A., Griffin, D.J., Tang, X., Kim, Y., and Rousseau, R.W. (2020). Optimal feedback control of batch self-assembly processes using dynamic programming. *Journal of Process Control*, 88, 32–42. doi: https://doi.org/10.1016/j.jprocont.2020.01.013.

Hermanto, M.W., Braatz, R.D., and Chiu, M.S. (2011). Integrated batch-to-batch and nonlinear model predictive control for polymorphic transformation in pharmaceutical crystallization. *AIChE journal*, 57(4), 1008–1019. doi:https://doi.org/10.1002/aic.12331.

Jha, S., Karthika, S., and Radhakrishnan, T. (2017). Modelling and control of crystallization process. *Resource-Efficient Technologies*, 3(1), 94–100. doi: http://dx.doi.org/10.1016/j.reffit.2017.01.002.

Kalbasenka, A.N., Huesman, A.E., and Kramer, H.J. (2012). Model predictive control. *Industrial Crystallization Process Monitoring and Control*, 185–201.

Kim, Y. (2021). *Development of Optimal Control Methods for Unseeded Batch Cooling Crystallization: Combination of First-Principle and Machine-Learning Approaches*. Ph.D. thesis, Georgia Institute of Technology.

Kim, Y., Kawajiri, Y., Rousseau, R.W., and Grover, M.A. (2023). Modeling of nucleation, growth, and dissolution of paracetamol in ethanol solution for unseeded batch cooling crystallization with temperature-cycling strategy. *Industrial & Engineering Chemistry Research*, 62(6), 2866–2881. doi: https://doi.org/10.1021/acs.iecr.2c03465.

Lewis, A., Seckler, M., Kramer, H., and van Rosmalen, G. (2015). *Industrial Crystallization: Fundamentals and Applications*. Cambridge University Press. doi: https://doi.org/10.1017/CBO9781107280427.

Lima, F.A.R., Rebello, C.M., Costa, E.A., Santana, V.V., de Moares, M.G., Barreto, A.G., Secchi, A.R., de Souza, M.B., and Nogueira, I.B. (2023a). Improved modeling of crystallization processes by universal differential equations. *Chemical Engineering Research and Design*. doi: https://doi.org/10.1016/j.cherd.2023.11.032.

Lima, F.A.R.D., Faria, R.d.R., Curvelo, R., Cadorini, M.C.F., Echeverry, C.A.G., de Souza, M.B., and Secchi, A.R. (2023b). Influence of estimators and numerical approaches on the implementation of nmpcs. *Processes*, 11(4). doi:https://doi.org/10.3390/pr11041102.

Lima, F.A.R.D., Moraes, M.G.F., Secchi, A.R., and Souza Jr., M.B. (2022). Development of a recurrent neural networks-based nmpc for controlling the concentration of a crystallization process. *Digital Chemical Engineering*, 5, 100052. doi: https://doi.org/10.1016/j.dche.2022.100052.

Meng, Y., Yu, S., Zhang, J., Qin, J., Dong, Z., Lu, G., and Pang, H. (2019). Hybrid modeling based on mechanistic and data-driven approaches for cane sugar crystallization. *Journal of food engineering*, 257, 44–55. doi:https://doi.org/10.1016/j.jfoodeng.2019.03.026.

Moraes, M.G., de Souza Jr, M.B., and Secchi, A.R. (2018). Dynamics and MPC of an evaporative continuous crystallization process. In *Computer Aided Chemical Engineering*, volume 43, 997–1002. doi: https://doi.org/10.1016/B978-0-444-64235-6.50175-3.

Nagy, Z.K. (2009). Model based robust control approach for batch crystallization product design. *Computers & Chemical Engineering*, 33(10), 1685–1691. doi: https://doi.org/10.1016/j.compchemeng.2009.04.012.

Nagy, Z.K. and Braatz, R.D. (2003). Robust nonlinear model predictive control of batch processes. *AIChE Journal*, 49(7), 1776–1786. doi: https://doi.org/10.1002/aic.690490715.

Nagy, Z.K. and Braatz, R.D. (2012). Advances and new directions in crystallization control. *Annual review of chemical and biomolecular engineering*, 3, 55–75. doi:https://doi.org/10.1146/annurev-chembioeng-062011-081043.

Szilágyi, B., Agachi, P.S., and Nagy, Z.K. (2018). Chord length distribution based modeling and adaptive model predictive control of batch crystallization processes using high fidelity full population balance models. *Industrial & Engineering Chemistry Research*, 57(9), 3320–3332. doi:https://doi.org/10.1021/acs.iecr.7b03964.

Venkatasubramanian, V. (2019). The promise of artificial intelligence in chemical engineering: Is it here, finally? *AIChE Journal*, 65(2), 466–478. doi: https://doi.org/10.1002/aic.16489.

Wang, L., Zhu, Y., and Gan, C. (2023). Nonlinear model predictive control of crystal size in batch cooling crystallization processes. *Journal of Process Control*, 128, 103020. doi: https://doi.org/10.1016/j.jprocont.2023.103020.

Xiouras, C., Cameli, F., Quilló, G.L., Kavousanakis, M.E., Vlachos, D.G., and Stefanidis, G.D. (2022). Applications of artificial intelligence and machine learning algorithms to crystallization. *Chemical Reviews*, 122(15), 13006–13042. doi: https://doi.org/10.1021/acs.chemrev.2c00141.

Zheng, Y., Wang, X., and Wu, Z. (2022a). Machine learning modeling and predictive control of the batch crystallization process. *Industrial & Engineering Chemistry Research*, 61(16), 5578–5592. doi: https://doi.org/10.1021/acs.iecr.2c00026.

Zheng, Y., Zhao, T., Wang, X., and Wu, Z. (2022b). Online learning-based predictive control of crystallization processes under batch-to-batch parametric drift. *AIChE Journal*, 68(11), e17815. doi: https://doi.org/10.1002/aic.17815.